Submission to ACS Sustainable Chemistry & Engineering

Page: 10; Figure: 5; Table: 0.

Supporting Information

In-situ fabrication of electro-Fenton catalyst from Fe^{2+} in acid mine drainage: Influence of coexisting metal cations

Yi-Meng Sun, Lin-Feng Zhai*, Ming-Feng Duan, Min Sun*

Anhui Province Key Laboratory of Advanced Catalytic Materials and Reaction,

School of Chemistry and Chemical Engineering, Hefei University of Technology,

Hefei, 230009, China

* **Corresponding author**:

Dr. Lin-Feng Zhai

Tel: +086-551-2901450;

E-mail: linfengzhai@hfut.edu.cn

Dr. Min Sun

Tel: +086-551-2901450;

E-mail: sunmin81@mail.ustc.edu.cn

The following is included as supporting information for this paper:

coexisting metal ions in the AMDs are (a) Co^{2+} and Mn^{2+} at 7 mM; (b) Co^{2+} and Mn^{2+} at 0.7 mM; (c) no coexisting metal ion; (d) Co^{2+}, Mn^{2+}, Ni^{2+} and Zn^{2+} at 7 mM; (e) Co^{2+}, Mn^{2+}, Ni^{2+} and Zn^{2+} at 0.7 mM; (f) Co^{2+}, Mn^{2+}, Ni^{2+}, Zn^{2+}, Cu^{2+} and Al^{3+} at 7 mM; and (g) Co^{2+}, Mn^{2+}, Ni^{2+}, Zn^{2+}, Cu^{2+} and Al^{3+} at 0.7 mM.

Page S10 **Figure S5.** Metal contents in the composites prepared from real AMD I and AMD II. The inset displays TG curves of the composites.

Section S1. Methods on structure characterization and electrochemical analysis of the Fe_3O_4/GF composite. Meal contents in the Fe_3O_4/GF composite were determined by thermogravimetry (TG) on a TGA DT-50 apparatus (Shimadzu, Japan) and X-ray fluorescence spectrometry (XRF) on an XRF-1800 apparatus (Shimadzu, Japan). Microscopic image of the composite and energy-dispersive X-ray spectroscopy (EDX) elemental mapping were obtained on a field emission gun scanning electron microscope (FEGSEM) (Zeiss Sigma, Germany). Valence states of metals were characterized by X-ray photoelectron spectroscopy (XPS) on an ESCALAB 250 spectrometer (Thermo, USA) equipped with a monochromatic Mg Kα X-ray source (1253.6 eV). Crystalline phases of metals were identified by X-ray diffractogram (XRD) using a Bruker D8 advance X-ray diffractometer (Germany) equipped with graphite-monochromated Cu Kα radiation (λ = 1.54178 Å). The composites were cut into 5 × 5 mm^2 pieces for SEM and XRD analyses, and were ground into powders for TG and XPS analyses.

Electrochemical impedance spectroscopy (EIS) was performed on a CHI 660D electrochemical workstation (CH Instruments Inc., USA), with the prepared Fe_3O_4/GF composite used as working electrode, Pt as counter electrode and saturated calomel electrode (SCE) as the reference. The electrolyte was 50 mM Na_2SO_4 containing 25 mg L^{-1} RhB at pH 7.0. The frequency of the AC signal varied from 100 kHz to 0.01 Hz with potential amplitude of 5 mV at the open circuit potential. Scanning electrochemical microscopy (SECM) was carried out on a Sensolytics SECM (Germany) in three-electrode mode. The SECM tip (working electrode) was a

25 μm Pt microelectrode, the reference electrode was Ag/AgCl, and the counter electrode was a platinum wire. The substrate was nickel foam loaded with Fe_3O_4/GF composite powder. To prepare the substrate, a mixture of 95 wt% of Fe_3O_4/GF composite and 5 wt% of polyvinylidene fluoride (PVDF) was ground with an appropriate amount of N-methyl-2-pyrrolidone (NMP) for 30 min to obtain a black paste. The paste was then cast on the nickel foam and dried in a vacuum oven at 50 °C overnight. The obtained nickel foam was pressed at 10 MPa for 1 min. The electrolyte consisted of 0.1 M KCl and 5 mM $[Fe(CN)_6]^{4-}$, and the tip potential was set at +500 mV to initiate the oxidation of $[Fe(CN)_6]^{4-}$. Scans were conducted both vertically and parallel above the surface of substrate at a rate of 10 μm s^{-1}. The interval between two data points was 12.5 μm, and the surface map of an area 200 × 200 μm was measured using the positive feedback mode.

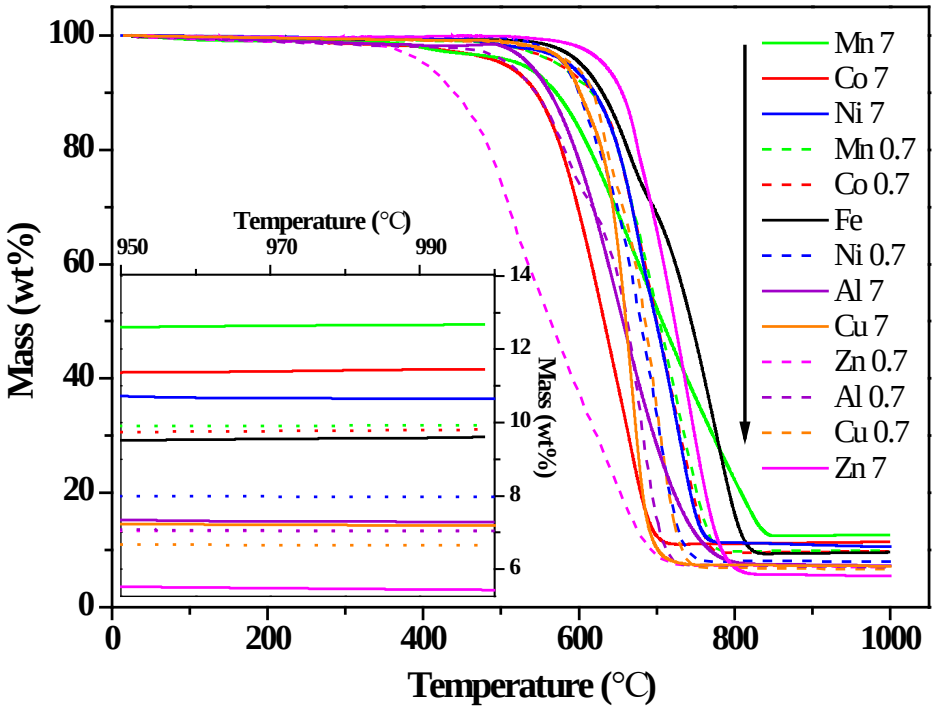

Figure S1. TG curves of the composites prepared from different synthetic AMDs. The inset displays the TG curves in the temperature range of 950 to 1000 °C.

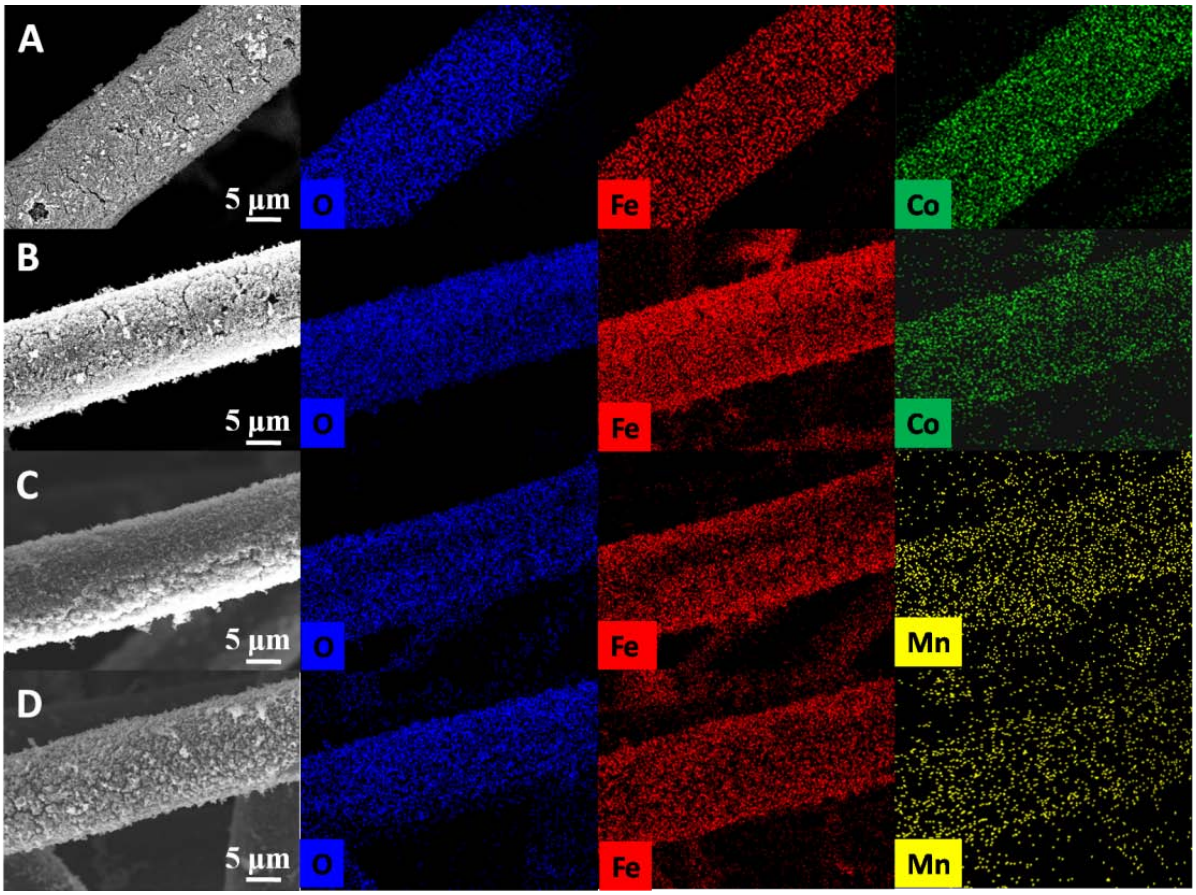

Figure S2. SEM images and elemental mappings of the composites prepared from synthetic AMDs with (A) 7 mM Co^{2+}; (B) 0.7 mM Co^{2+}; (C) 7 mM Mn^{2+}; or (D) 0.7 mM Mn^{2+} as coexisting metal cation.

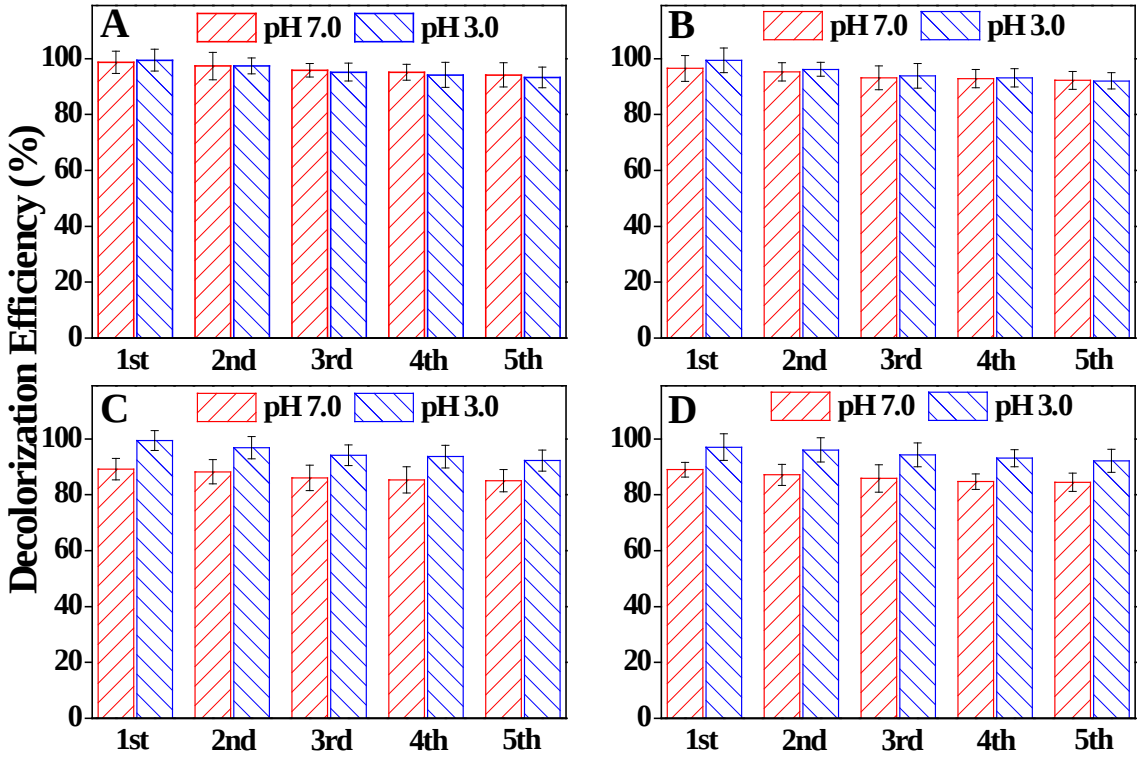

Figure S3. Decolorization efficiencies of RhB in five successive cycles at the composite cathodes prepared from synthetic AMDs with (A) 7 mM Co^{2+}; (B) 7 mM Mn^{2+}; (C) 0.7 mM Co^{2+}; or (D) 0.7 mM Mn^{2+} as coexisting metal cation.

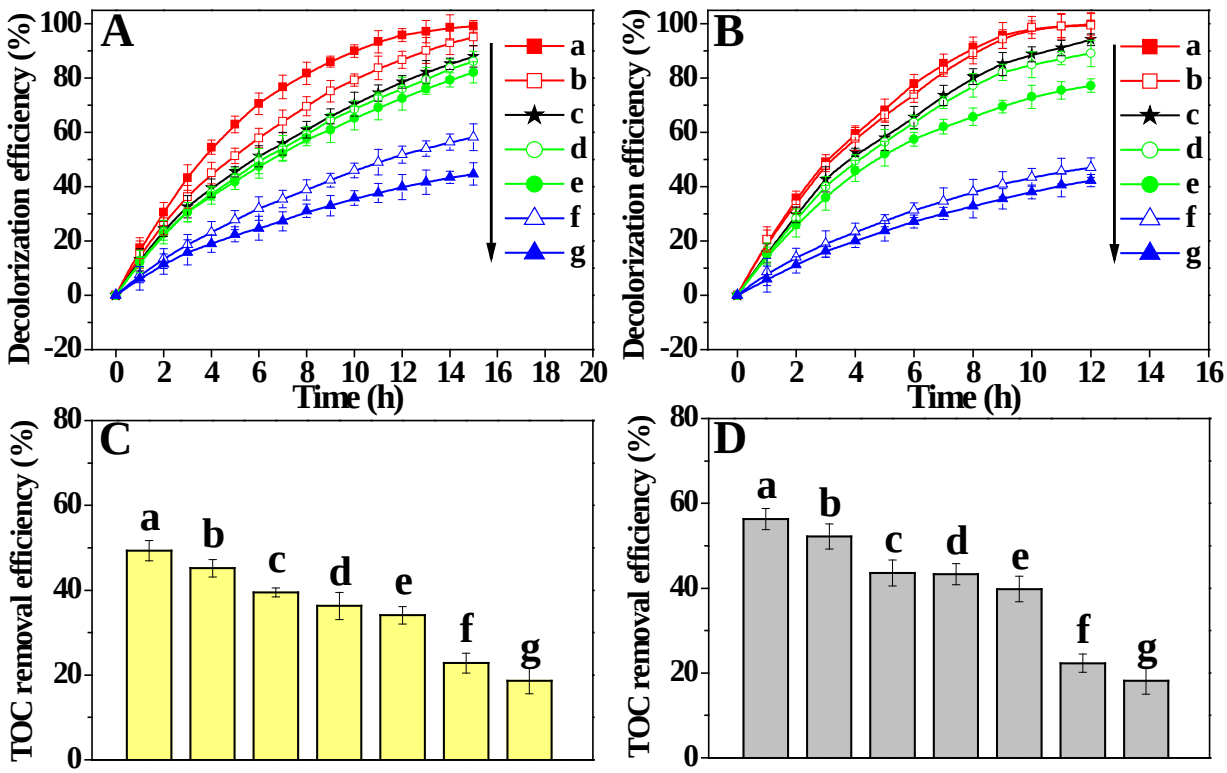

Figure S4. Decolorization efficiencies of RhB in the (A) pH 7.0 and (B) pH 3.0 EF systems; TOC removal efficiencies of RhB solution after (C) 15 h of degradation at pH 7.0 and (D) 12 h of degradation at pH 3.0 at the composite cathodes prepared from different synthetic AMDs. The coexisting metal ions in the AMDs are (a) Co^{2+} and Mn^{2+} at 7 mM; (b) Co^{2+} and Mn^{2+} at 0.7 mM; (c) no coexisting metal ion; (d) Co^{2+}, Mn^{2+}, Ni^{2+} and Zn^{2+} at 7 mM; (e) Co^{2+}, Mn^{2+}, Ni^{2+} and Zn^{2+} at 0.7 mM; (f) Co^{2+}, Mn^{2+}, Ni^{2+}, Zn^{2+}, Cu^{2+} and Al^{3+} at 7 mM; and (g) Co^{2+}, Mn^{2+}, Ni^{2+}, Zn^{2+}, Cu^{2+} and Al^{3+} at 0.7 mM.

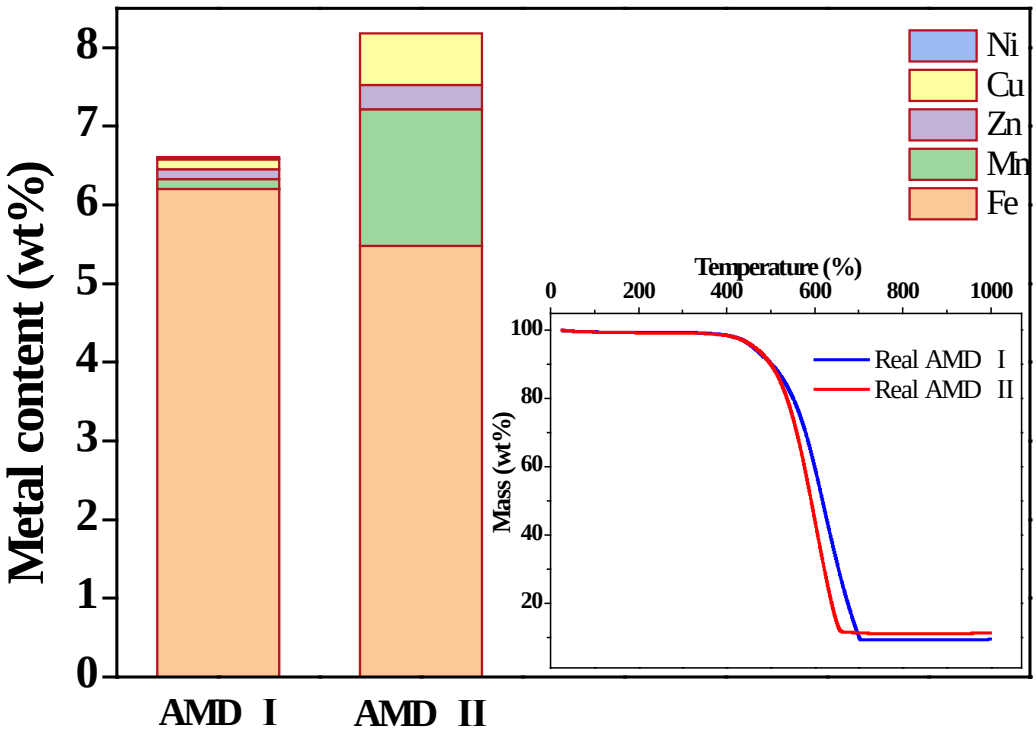

Figure S5. Metal contents in the composites prepared from real AMD I and AMD II. The inset displays TG curves of the composites.